J. Fluid Mech. (2015), *vol.* 771, *pp.* 327–340. © Cambridge University Press 2015
doi:10.1017/jfm.2015.177

Detachment of droplets from cylinders in flow using an experimental analogue

C. J. Hotz[1,2], R. Mead-Hunter[2,3,†], T. Becker[4], A. J. C. King[2], S. Wurster[1], G. Kasper[1] and B. J. Mullins[2,3]

[1]Institute for Mechanical Process Engineering and Mechanics, Karlsruhe Institut fuer Technologie, D-76131, Karlsruhe, Germany

[2]Fluid Dynamics Research Group, Curtin University, GPO Box U1987, Perth WA 6845, Australia

[3]Health, Safety and Environment, School of Public Health, Faculty of Health Sciences, Curtin University, GPO Box U1987, Perth WA 6845, Australia

[4]Nanochemistry Research Institute, Curtin University, GPO Box U1987, Perth WA 6845, Australia

(Received 25 October 2013; revised 6 March 2015; accepted 17 March 2015;
first published online 20 April 2015)

This work experimentally examines the detachment of liquid droplets from both oleophilic and oleophobic fibres, using an atomic force microscope. The droplet detachment force was found to increase with increasing fibre diameter and forces were higher for philic fibres than phobic fibres. We also considered the detachment of droplets situated on the intersection of two fibres and arrays of fibres (such as found in fibrous mats or filters) and found that the required detachment forces were higher than for similarly sized droplets on a single fibre, though not as high as expected based on theory. A model was developed to predict the detachment force, from single fibres, which agreed well with experimental results. It was found that the entire dataset (single and multiple fibres) could be best described by power law relationships.

Key words: breakup/coalescence, bubble dynamics, drops and bubbles

1. Introduction

The formation and behaviour of liquid droplets represents an interesting case in fluid dynamics, where a discrete parcel of fluid (in a multiphase fluid system) may spread, roll, deform or break up due to the application of external forces. Droplet dynamics has received significant attention in the literature, whether it be due to shape (Aussillous & Quere 2004), behaviour (Andrieu *et al.* 2002; Bach, Koch & Gopinath 2004), or interactions with a particular surface (Bayer & Megaridis 2006; Savva & Kalliadasis 2013).

Furthermore, the behaviour of droplets on fibres is of interest in a number of fields, including interface, textile and separation science, with applications as wide ranging as multiphase fluid separation, fuel cells, batteries, and biomedical ‘scaffolds’. While wetting behaviour on flat plates has been well studied, there have been comparatively few works that consider droplets on cylindrical elements (such as fibres) (Carroll

†Email address for correspondence: r.mead-hunter@curtin.edu.au

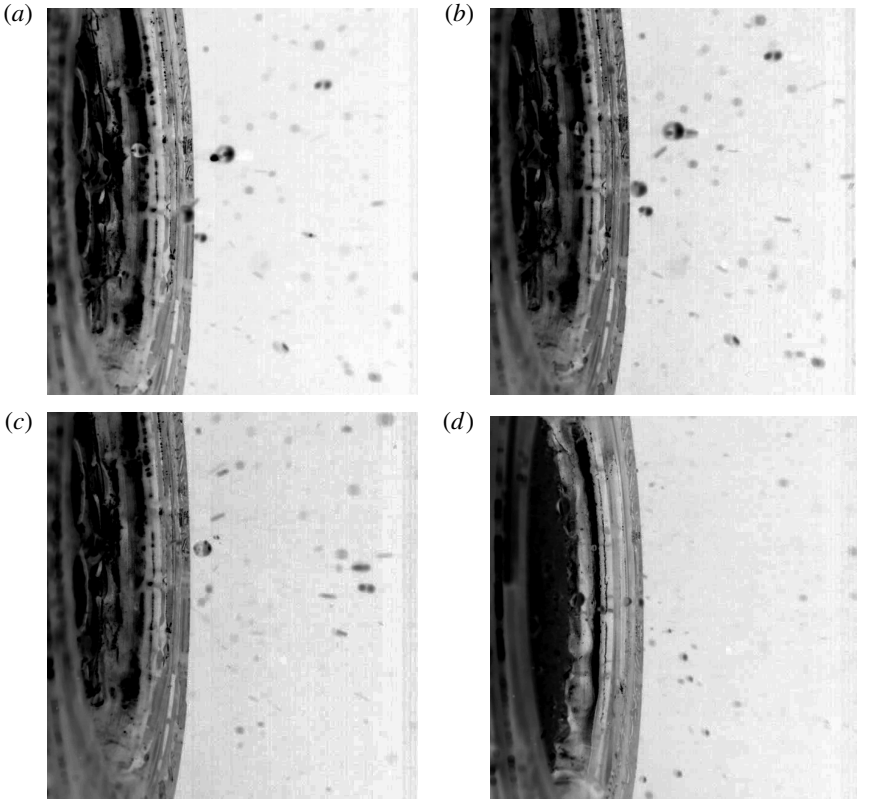

FIGURE 1. Droplet detachment from the downstream face of filters: (*a–c*) successive images of detachment from a saturated oleophilic oil mist filter (0.024 s between images) and (*d*) detachment from a saturated oleophobic oil mist filter. All filters are microfibre glass media (randomly oriented arrays of fibres).

1976, 1984, 1986; Quere, Di Meglio & Brochard-Wyart 1988; McHale *et al.* 1997; McHale & Newton 2002; Lorenceau & Quere 2004; Mullins *et al.* 2005, 2006; Gilet, Terwagne & Vandewalle 2009, 2010; Mead-Hunter *et al.* 2011, 2012*a*).

Similarly, the detachment of droplets from cylindrical elements has received relatively little attention, with the detachment of droplets from micro-structures (Hao, Lu & Yao 2013) and super-hydrophobic surfaces (Farhangi *et al.* 2012) receiving the most recent interest.

There are a number of recent works, however, both fundamental (Leal *et al.* 2009; de Ruiter *et al.* 2012) and applied (Gauthier *et al.* 2012; Sahu *et al.* 2013), which have turned their attention to the detachment of droplets from fibres. As well as being an interesting physical process in itself, the detachment of droplets from fibres has applications in fuel cell and coalescence filtration technology among other fields. It is the process of the detachment of droplets from filter fibres that is the motivation for this work. Such a process is illustated in figure 1, with the images obtained by the authors using a high-speed camera, using glass-fibre media and di-ethyl-hexyl sebacate (Sigma Aldrich).

Coalescence or mist filtration represents an interesting multiphase fluid flow case. Where the flow occurs within a complex (open) porous medium composed of fine

cylindrical fibres. Such systems are usually composed of <5 % filter fibres (i.e. >95 % void space), though in operation up to 80 % of the void space can fill with liquid, impeding the passage of air/gas through the filter.

In terms of coalescence filtration, understanding the behaviour of droplets on individual fibres could potentially lead to improved filter designs. Work in this area has consisted of both experiments (Dawar *et al.* 2006; Dawar & Chase 2008; Sahu *et al.* 2013) and simulations (Gac & Gradon 2012; Mead-Hunter, King & Mullins 2012*b*) of droplet fibre systems.

A detailed understanding of droplet detachment will be critical in accurately describing entrainment, which is a significant problem in many mist filter systems. This is a process whereby liquid collected by a coalescing filter may be reintroduced to an air stream in the form of large (on the order of ∼100 μm diameter) droplets. The entrainment of droplets will typically occur when the flow forces are high enough to cause a droplet to detach from a filter fibre or fibres. Such forces are difficult to measure *in situ* due to the broad spectrum of droplet sizes and trajectories (as evidenced by figure 1, not to mention gas flow paths through the filter, which is mainly void space, though this can be fluid filled).

In reality, aerosol generation from such systems is likely to be a combination of bubble bursting and droplet detachment; however we will consider the simplest case, that of droplet detachment, as a first option. To date, only one previous work (Mullins *et al.* 2007) has measured the force required to detach droplets from fibres. In their work, Mullins *et al.* (2007) demonstrated that such measurements are feasible, and produced preliminary data. This work further develops the previous methodology, to allow the force required to detach droplets from fibres with differing wettabilities and multiple fibres to be examined experimentally.

As both oleophilic and oleophobic media are used in coalescing filters, detachment of both axisymmetric ('barrel') and asymmetric ('clamshell') shaped droplet conformations will be considered. The atomic force microscope will, therefore be used in this work to allow the accurate measurement of the force required to detach droplets from fibres.

It is hoped this work will expand the body of knowledge on such multiphase fluid systems.

2. Model

The force required to detach a droplet from a surface will be dependent on the wettability of the surface (as indicated by contact angle θ_c), the length of the contact line (L), and the surface tension of the liquid (σ). In the absence of an engineered surface (i.e. one with a defined microstructure or surface energy), the only parameter to change in the detachment process will be the length of the contact line, which will decrease as the droplet is drawn away from the surface. The force required to detach a droplet from a surface (F), therefore needs to be sufficient to overcome the force holding the droplet in place,

$$F > \sigma L \cos\theta_c, \tag{2.1}$$

and be applied sufficiently long to overcome any deformation (i.e. completely detaching the droplet). The point where detachment occurs would then correspond to the point where the length of the contact line reduces to zero. Therefore, the process of droplet detachment can be described as a change in length of contact line with time,

$$F = f\left(\frac{\mathrm{d}L}{\mathrm{d}t}\right). \tag{2.2}$$

This will be the process whether the detachment is from a non-wettable fibre or a flat plate. In the case of a droplet sitting on a wettable fibre, intersecting fibres, or a fibre mat, the same process occurs; though is complicated by the presence of multiple, discontinuous contact lines. The force required to detach droplets from these surfaces will also be a function of $\mathrm{d}L/\mathrm{d}t$; however these will each approach L values of zero, at different times. In the case of two intersecting fibres, the droplet will detach first from the lower fibre and then the overlapping fibre.

For a given system of monodisperse fibres,

$$F = nF_i, \tag{2.3}$$

where n is the number of fibres with which the droplet is in contact.

Ultimately, in the case of fibrous filters, droplet detachment will be driven by flow and will therefore be driven by drag forces acting on the droplet. The drag force (F_d) must overcome other forces in order for detachment to occur, such that

$$F_d \geqslant F_i. \tag{2.4}$$

Due to the influence of fibres and other droplets on the flow field it is likely that

$$F_d > nF \tag{2.5}$$

to induce detachment for droplets which are attached to multiple fibres.

Given the complex nature of the contact lines in the case of a fibrous mat, there may also be a need to consider additional factors, such as the effects of contact line pinning, and the surface structure itself (i.e. the presence of any inhomogeneities on the fibre surface). These factors may influence the adhesion forces present, and potentially will be in greater effect for systems with multiple fibres. Additionally, in many cases the droplet shape will deviate further from spherical the more fibres it intersects. This will change the direction of forces and hence overall magnitude. However, such complexity cannot be readily addressed for disordered arrays of fibres.

To aid analysis of the experiments, a model was developed to describe the detachment of a droplet from a fibre, allowing peak detachment forces to be calculated. This model was developed in addition to the one presented in Mullins *et al.* (2007) which was derived to be independent of contact angle. Since previous work (Mead-Hunter *et al.* 2012*a*) has found that static contact angles on flat plates may offer a reasonable approximation of the contact angles of 'clamshell' droplets on fibres, a new model has been developed, which uses a discrete integration to determine the length of the contact line.

Initially, a sphere of a defined volume is considered. This sphere is imposed on a cylinder, without considering any interaction, as shown in figure 2. We then create a cube of 8000 equal-volume cells which encloses the sphere and the fibre. This sphere of known volume may then be manipulated (by changing the axial dimensions) to take on an elliptical geometry, corresponding to the dimensions of a measured droplet on a fibre.

The conditions

$$\frac{x^2}{a^2} + \frac{y^2}{b^2} + \frac{z^2}{c^2} < 1 \tag{2.6}$$

and

$$x^2 + (y - D)^2 > R^2, \tag{2.7}$$

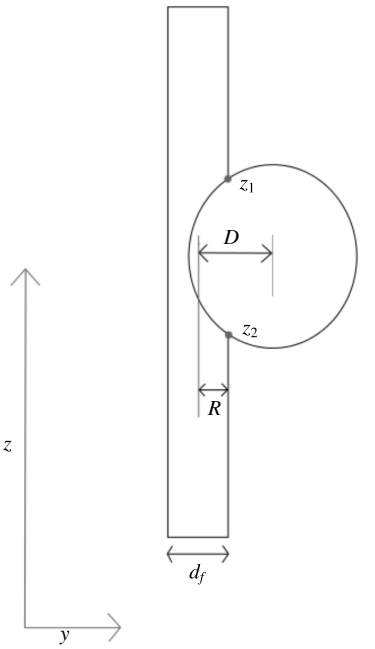

FIGURE 2. Schematic representation of a droplet on a fibre, showing the definition of model parameters. Detachment is perpendicular to the fibre axis.

define the volume of the drop, where x, y and z are Cartesian coordinates, a, b and c minor axes of the ellipsoid, R the radius of the cylinder and D the distance in the y direction from the longitudinal axis to the origin. The cylinder is oriented along the z-axis.

On the basis of (2.6) and (2.7) each equal-volume cell is identified as being within the sphere, the cylinder, or both. Only the cells in the cube which are inside the sphere and outside the cylinder are part of the liquid volume. The liquid volume is then determined by multiplying the number of cells making up the liquid volume by the volume of an individual cell. The axial dimensions of the sphere/ellipsoid can then be adjusted such that the desired drop volume is obtained.

The location of the contact lines may be found by applying the condition $x = 0$, $y = D - R$, to

$$\frac{x^2}{a^2} + \frac{y^2}{b^2} + \frac{z^2}{c^2} = 1, \tag{2.8}$$

giving

$$z_{1,2} = \pm c\sqrt{1 - \left(\frac{(D-R)^2}{b^2}\right)}. \tag{2.9}$$

where z_1 and z_2 are the end points of the contact lines, as illustrated in figure 2.

The wetted length is then the distance between the two values of z obtained. The total length of the contact line can then be found by determining the corresponding x and y coordinates. This is performed using 20 000 discrete z points and evaluating the y values by substituting

$$x^2 + (y - D)^2 = R^2 \tag{2.10}$$

into (2.8) such that

$$y = -\frac{Db^2}{a^2 - b^2} \pm \sqrt{\frac{D^2 b^4}{(a^2 - b^2)^2} + \frac{b^2(R^2 - D^2)c^2 - a^2 b^2(z^2 - c^2)}{(a^2 - b^2)c^2}}. \tag{2.11}$$

The corresponding x values may then be found using (2.10).

The length of the contact line (L) may then be found by connecting all the accumulated points forming the contact line, such that

$$L = 2\sum_{i=1}^{n} \sqrt{(x_i - x_{i-1})^2 + (y_i - y_{i-1})^2 + (z_i - z_{i-1})^2}, \tag{2.12}$$

including a factor of 2, due to the symmetric nature of the contact line.

In cases where D is small, parts of the cylinder will be enclosed by the droplet (when $D = 0$, the droplet is axisymmetric) and the contact line will be interrupted and will form two lines around the cylinder. This case is detected when (2.11) produces complex results. These complex results are deleted from the model.

The force caused by the line tension has a defined direction and acts towards the centre of the cylinder. Therefore, both axisymmetric and 'clamshell' shaped droplets in their equilibrium positions will have no resultant force. Following on from previous work (Mead-Hunter *et al.* 2011), the detachment force will be of the form

$$F = \sigma \int_L \hat{\boldsymbol{v}} \cos(\theta) \mathrm{d}L \tag{2.13}$$

where σ is the surface tension of the liquid, θ is the contact angle and, $\hat{\boldsymbol{v}}$ is a unit vector between the contact line and the longitudinal axis of the cylinder. Such a unit vector has been derived in previous work (Mead-Hunter *et al.* 2011).

The force required to detach a droplet from a cylinder may then be found using

$$F = \sigma \int_0^N \hat{\boldsymbol{v}} \cos(\theta) \mathrm{d}L, \tag{2.14}$$

where N is the number of discrete points of z.

The theoretical model was developed and implemented using MATLAB (MathWorks).

3. Experiment

The direct measurement of droplet detachment from fibres in a flow field would be challenging, and any system used would probably alter the flow field and affect the results. To avoid such challenges, the detachment is measured in the absence of a flow field using an atomic force microscope (AFM). This was achieved by drawing the droplet away from the fibre using the AFM cantilever. As the flow in a filter is typically unidirectional (especially when considering a single fibre), drawing the droplet away from the fibre is analogous to the drop being 'blown off' the downstream side in the presence of flow. Such methods have previously been used to assess the motion of droplets moving along a fibre (Mead-Hunter *et al.* 2011).

In order to allow the detachment forces of oil droplets to be measured, modified cantilevers had to be prepared in a manner similar to those used in previous work by Mead-Hunter *et al.* (2011). The key difference was that in this work the cantilevers

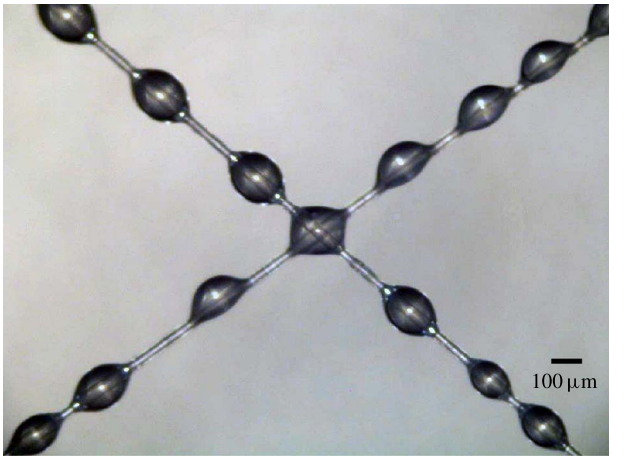

FIGURE 3. Coalesced droplets on two intersecting fibres.

(NSC-14,15, μmasch, Tallinn, Estonia), were first coated with a fluorinated co-polymer (TL1143, Thor Chemie, Speyer, Germany) to render them oleophobic before glass spheres were attached, and the spheres subsequently coated with the polymer. The cantilevers were prepared using a Dimension 3000 Atomic Force Microscope (Veeco, Camarillo, USA). Cantilevers were calibrated using the Sader method (Sader, Chon & Mulvaney 1999).

Fibres were placed in custom stainless steel mounts and cleaned before use, by immersion in ethanol in an ultrasonic bath. Given that the fibres were oleophilic as supplied, fibres for oleophobic experiments had to be prepared by coating the clean fibres with the same fluorinated co-polymer as used in the cantilever preparation, rendering them oleophobic and super-hydrophobic. This work utilised three configurations:

(i) single fibres;
(ii) an intersecting fibre geometry, where two fibres were arranged in the mount in a cross, as shown in figure 3;
(iii) whole, commercially manufactured non-woven fibrous filter media (fibre arrays), which were supplied in either oleophilic or (coated/treated) oleophobic form. Such a fibre array is shown in figure 4, where the filter media, with a schematic demonstrating how a droplet may be in contact with multiple fibres.

Fibres were loaded by exposure to an oil aerosol generated by a Collison type nebuliser. Both di-ethyl-hexyl-sebacate (DEHS, Sigma-Aldrich, Australia) and glycerol (Sigma-Aldrich, Australia) were used. Given the need for discrete droplets, the whole of the filter (fibre arrays) was not loaded in this manner, and instead had individual oil droplets added to the surface using an AFM probe. The properties of the materials used in this work are shown in table 1.

Measurements of droplet detachment were conducted using a PicoPlus 3000 (Agilent Technologies) scanning probe microscope (SPM), with a large-range multipurpose AFM scanner, and Newport 423 series motorised x-y-z stage. This configuration is shown in figure 5. Given that the distance the cantilever must move away from the fibre/filter in order to detach a droplet was greater than the vertical measurement range of the AFM, measurements were achieved by moving the fibre away from the

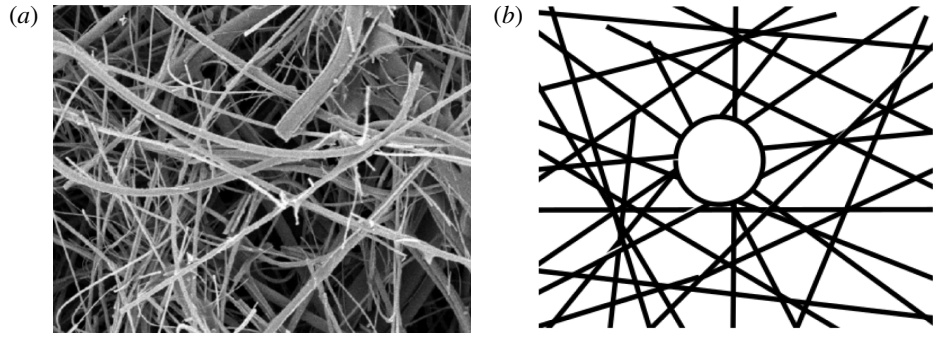

FIGURE 4. Scanning electron microscope image of an oleophobic glass fibre array (fibrous filter) (*a*) and a schematic showing a droplet sitting on the surface of the fibrous mat (*b*). It can be seen that the droplet may be in contact with multiple fibres. The stainless steel fibre arrays used were composed of monodisperse fibre diameters, while all glass media were polydisperse.

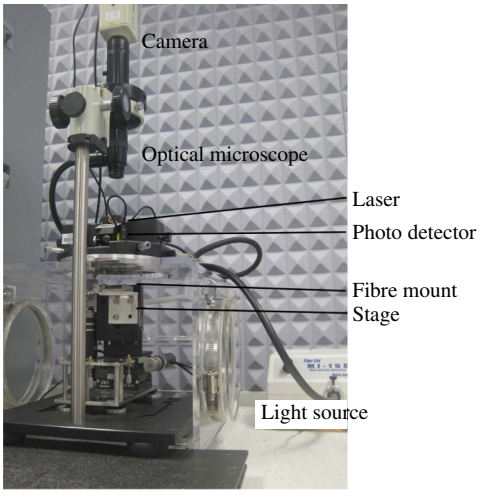

FIGURE 5. (Colour online) The experimental apparatus used to conduct the measurements.

cantilever, using the *x*-*y*-*z* stage. This represents a significant improvement on the original methodology used by Mullins *et al.* (2007).

4. Results and discussion

All droplets were measured multiple times by re-attaching the droplet to the fibre after each detachment measurement. This allowed the detachment force to be measured to a higher certainty for each droplet and also the same droplet to be measured at multiple locations on each fibre.

The results for single fibres are shown in figure 6, where the measured force has been normalised by the surface tension to allow results for both DEHS and glycerol to be plotted on the same graph. Using these values allows a single model line for all data to be included on each graph. It should be noted, however, that variables such as

Fibres

Material	Abbreviation	d_f (μm)
Polyester	PSF	5.4, 11.2, 13, 21, 27, 34
Polyethylene	PE	22
Glass	G	10.8
Stainless steel	S	8

Fibrous mats

Material	Abbreviation	d_f (μm)
Stainless steel	S	2
Stainless steel	S	4
Stainless steel	S	8
Glass	G	3.63
Glass	G	0.67
Glass	G	0.66

Liquids

Liquid	Abbreviation	σ (N m^{-1})
DEHS	(D)	0.032
Glycerol	(G)	0.064

TABLE 1. Properties of the fibres, filters and liquids used in this work, where d_f is the fibre diameter.

fibre surface roughness, contact angle hysteresis and errors associated with the AFM measurements will all cause measured values to differ from model predicted values.

It can be seen that for both oleophilic and oleophobic fibres, the force required to detach a droplet increases with an increase in fibre diameter; this was expected as the contact line length increases with fibre diameter. Furthermore, comparison of figure 6(*a*) with 6(*b*) indicates that the force required to detach a droplet from an oleophilic fibre is significantly greater than that required to detach a droplet from an oleophobic fibre. It should be noted, however, that the axisymmetric droplets which formed on the oleophilic fibres were larger than the 'clamshell' shaped droplets that formed on the oleophobic fibres.

Two data points from Mullins *et al.* (2007) are shown in figure 6(*a*), and it can been seen that there is a reasonable agreement between these measurements and our measurements with DEHS on steel and glass fibres.

The results for the theoretical model are also shown in figure 6. The model has been evaluated for DEHS on PSF fibres, using contact angles obtained in previous work on the same fibre type (Mead-Hunter *et al.* 2011), which were found to vary with diameter. The model fit for both oleophilic and oleophobic fibres to the measured data for DEHS is relatively good, with R^2 values of 0.81 and 0.92, for oleophilic and oleophobic fibres, respectively. In the oleophilic case it can be seen that the model line is also a reasonable fit to the measurements on glycerol droplets. This is not the case for the oleophobic fibres, where some deviation exists. It has been observed that while the axisymmetric droplets appear similar in shape, there is an observable difference in the appearance of DEHS and glycerol droplets on the oleophobic fibres, which appear to be more easily wetted by DEHS. This is also supported by previous work where

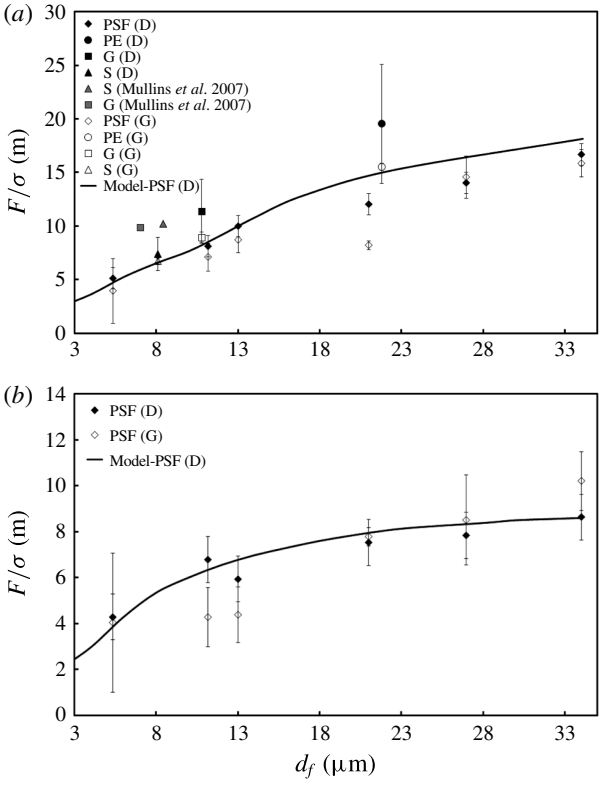

FIGURE 6. Measured detachment forces for (*a*) single oleophilic fibres and (*b*) single oleophobic fibres. In the legend (D) indicates measurements performed with DEHS and (G), those with glycerol; see table 1 for other abbreviations. The solid lines indicate the model predictions.

the contact angles of DEHS and glycerol on flat surfaces coated with the polymer were measured and found to differ by ∼25° (Mead-Hunter *et al.* 2012*a*).

The measurements taken on the intersecting fibre geometries and the filter materials are shown in figure 7, with the model curves for single fibres. To allow all measurements to be plotted in one graph, a value equal to twice the maximum available fibre circumference, termed L_p, was calculated for all measurements. This is defined as

$$L_p = 2\sum_i (C_1 + C_i)\,, \tag{4.1}$$

where i represents the number of fibres with which the droplet is in contact and $C_1 = \pi d_f$.

This is the approximate length of contact line that would exist if all droplets were perfectly axisymmetric and the fibre completely smooth (i.e. a contact line perpendicular to the fibre axis). For a single fibre this is $2\pi d_f$ and for two intersecting fibres becomes $4\pi d_f$. For the non-woven fibrous mats the length L_p was calculated based on the number of fibres likely to be in the vicinity of the droplet. This was determined by considering a droplet of average size (85 μm in this case) and calculating the maximum cross-sectional area of the droplet, then determining the

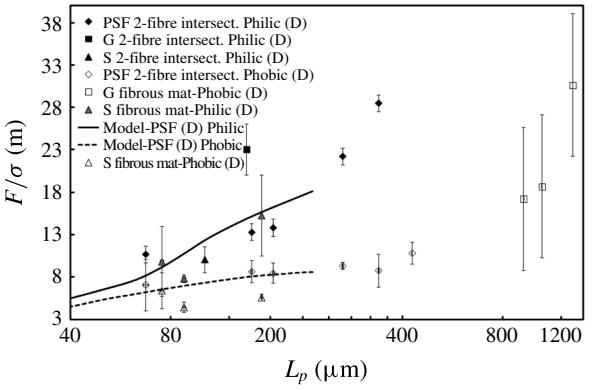

FIGURE 7. Measured detachment forces for droplets on intersecting/multiple fibres. The model lines for single fibres are also shown to illustrate the difference between single and multiple fibres.

maximum number of fibres (multiples of $2\pi d_f$) that the droplet could be in contact with, based on the packing density of the filter.

Generally, the force required to detach droplets from intersecting oleophilic fibres was found to be 77 % higher than the force needed to remove droplets from a single oleophilic fibre of the same diameter. For oleophobic fibres, the detachment from fibre intersections was only 32 % higher than that for single fibres. The difference is attributed to the different wettabilities of the fibres, with the possibility that the underlying fibre only contacted a small portion of the droplet in comparison to the oleophilic case. However, in both cases the force required to detach a droplet from intersecting fibres was less than twice that required to detach a droplet from a single fibre, which was as initially expected (at least in the oleophilic case). As mentioned in § 2, distortion of droplets could influence results in the multiple fibre cases; however this effect cannot readily be quantified.

Figure 8 shows a plot of all measurements performed, separated into philic and phobic. The complete data sets can be approximated by power laws, where

$$\frac{F}{\sigma} = 1050 L_p^{0.47} \tag{4.2}$$

for the oleophilic fibres ($R^2 = 0.69$), and

$$\frac{F}{\sigma} = 223 L_p^{0.37} \tag{4.3}$$

for the oleophobic fibres ($R^2 = 0.79$), with L_p in units of metres (to ensure dimensional consistency). These power laws are shown in figure 8 and offered as they may be useful in assessing the detachment force for droplets on fibres and fibrous filters, without the need to evaluate (2.14) numerically. A power law fit was chosen, as this was found to agree with both experimental and model data in previous work on droplet motion along fibres (Mead-Hunter *et al.* 2011), which plotted similar parameters.

A power law relationship also describes the change in length of the contact line during the process of detachment. The detachment process draws a droplet away from the surface, reducing the length of the contact line until the droplet is detached

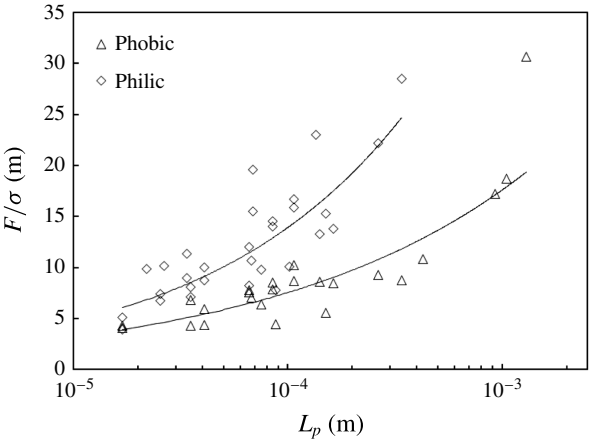

FIGURE 8. The complete dataset, showing the power law fits for philic and phobic media.

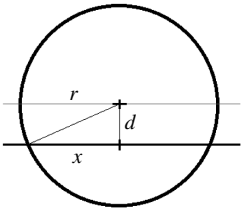

FIGURE 9. Schematic of the simplified case of a sphere traversing a plane.

(i.e. the force holding the droplet in place decreases as the length of contact line is reduced). This decreasing length of contact line as the droplet is being pulled away (displaced from the fibre) will eventually lead to detachment. Accurate determination of the length of the contact line and its subsequent reduction with displacement of the droplet is exceedingly complicated. Not only does the length of the contact line on a curved surface need to be determined, but the (largely unknown) deformation of the droplet and contact angle hysteresis during this process also need to be taken into account, as they also influence contact line length.

As we have incorporated force and surface tension together (the F/σ term in figure 8) and describe them as a function of length of contact line, we need only consider the length of contact line. We can consider a simplified case of a sphere moving away from an arbitrary fixed plane, initially located at a point transecting the centroid of the sphere, illustrated in figure 9. As the sphere is displaced, we can examine the effect on the length of the contact line. Initially, this will be defined by $2\pi r$, with r being the radius of the sphere. The contact line radius will decrease as the sphere is moved upwards and we denote this x. If we define d as the displacement, then as the sphere is moved up (i.e. d increases) the value of x will decrease resulting in a decrease in the length of contact line, defined as $2\pi x$. The length of contact line is therefore ultimately dependent on the value of x, which itself is related to the displacement, d. The value of x is defined by

$$x = (r^2 - d^2)^{1/2}. \tag{4.4}$$

As the length of the contact line is described by a power law, it seems reasonable that the force (which is itself a function of L_p) would also conform to a power law. Of course in a real case the shape of the droplet will change to some extent; however many other parameters are also changing simultaneously. If we consider our power law fits to the data, the powers are similar (0.5 versus 0.47 and 0.37), with variation likely to be due to the differences in geometry between our simplified case and more complicated real world geometries.

5. Conclusion

In this work, the force required to detach liquid droplets from oleophilic and oleophobic fibres was measured experimentally. The results indicate that the force required to detach a droplet from a fibre intersection is higher than to detach a droplet from a single fibre, though only 77 % higher for oleophilic fibres and 32 % higher for oleophobic fibres. We have also considered the detachment of droplets from intersecting fibres and filter materials and found that these forces are higher than for droplets on single fibres, but again not as high as expected. A theoretical model was developed which shows reasonable agreement with our single fibre measurements; however this model cannot be readily extended to more complex geometries. Empirical relationships based on the full experimental datasets were also developed and presented.

Acknowledgements

This work was funded by the Australian Research Council and the DAAD-ATN Travel Grant Scheme.

REFERENCES

ANDRIEU, C., BEYSENS, D. A., NIKOLAYEV, V. S. & POMEAU, Y. 2002 Coalescence of sessile drops. *J. Fluid Mech.* **453**, 427–438.

AUSSILLOUS, P. & QUERE, D. 2004 Shapes of rolling liquid drops. *J. Fluid Mech.* **512**, 133–151.

BACH, G. A., KOCH, D. L. & GOPINATH, A. 2004 Coalescence and bouncing of small aerosol droplets. *J. Fluid Mech.* **518**, 157–185.

BAYER, I. S. & MEGARIDIS, C. 2006 Contact angle dynamics in droplets impacting on flat surfaces with different wetting characteristics. *J. Fluid Mech.* **558**, 415–449.

CARROLL, B. J. 1976 The accurate measurement of contact angle, phase contact areas, drop volume, and Laplace excess pressure in drop-on-fiber systems. *J. Colloid Interface Sci.* **57** (3), 488–495.

CARROLL, B. J. 1984 The equilibrium of liquid drops on smooth and rough circular cylinders. *J. Colloid Interface Sci.* **97** (1), 195–200.

CARROLL, B. J. 1986 Equilibrium conformations of liquid drops on thin cylinders under forces of capillarity. A theory for the roll-up process. *Langmuir* **2**, 248–250.

DAWAR, S. & CHASE, G. G. 2008 Drag correlation for axial motion of drops on fibers. *Sep. Purif. Technol.* **66**, 6–13.

DAWAR, S., LI, H., DOBSON, J. & CHASE, G. G. 2006 Drag correlation of drop motion on fibers. *Drying Technol.* **24**, 1283–1288.

FARHANGI, M. M., GRAHAM, P. J., CHOUDHURY, N. R. & DOLATABADI, A. 2012 Induced detachment of coalescing droplets on superhydrophobic surfaces. *Langmuir* **28**, 1290–1303.

GAC, J. M. & GRADON, L. 2012 Modeling of axial motion of small dropets deposited on smooth and rough fiber surfaces. *Colloids Surf.* A **414**, 259–266.

GAUTHIER, T., HELLSTERN, E., KEVREKIDIS, I. G. & BENZINGER, J. 2012 Drop detachment and motion on fuel cell electrode materials. *ACS Appl. Mater. Interfaces* **4**, 761–771.

GILET, T., TERWAGNE, N. & VANDEWALLE, N. 2009 Digital microfluidics on a wire. *Appl. Phys. Lett.* **95**, 014106.

GILET, T., TERWAGNE, N. & VANDEWALLE, N. 2010 Droplets sliding on fibres. *Eur. Phys. J.* E **31**, 253–262.

HAO, P., LU, C. & YAO, Z. 2013 Droplet detachment by air flow for microstructured superhydrophobic surfaces. *Langmuir* **29**, 5160–5166.

LEAL, A. A., DEITZEL, J. M., MCKNIGHT, S. H. & GILLESPIE, J. W. JR. 2009 Interfacial behavior of high performance organic fibers. *Polymer* **50**, 1228–1235.

LORENCEAU, E. & QUERE, D. 2004 Drops on a conical wire. *J. Fluid Mech.* **510**, 29–45.

MCHALE, G., KAB, N. A., NEWTON, M. I. & ROWAN, S. M. 1997 Wetting of a high-energy fiber surface. *J. Colloid Interface Sci.* **186** (2), 453–461.

MCHALE, G. & NEWTON, M. I. 2002 Global geometry and the equilibrium shapes of liquid drops on fibers. *Colloids Surf.* A **206** (1–3), 79–86.

MEAD-HUNTER, R., BERGEN, T., BECKER, T., O'LEARY, R. A., KASPER, G. & MULLINS, B. J. 2012*a* Sliding/rolling phobic droplets along a fiber: measurement of interfacial forces. *Langmuir* **28**, 3483–3488.

MEAD-HUNTER, R., KING, A. J. C. & MULLINS, B. J. 2012*b* Plateau-Rayleigh instability simulation. *Langmuir* **28**, 6731–6735.

MEAD-HUNTER, R., MULLINS, B. J., BECKER, T. & BRADDOCK, R. D. 2011 Evaluation of the force required to move a coalesced liquid droplet along a fiber. *Langmuir* **27** (1), 227–232.

MULLINS, B. J., BRADDOCK, R. D., AGRANOVSKI, I. E. & CROPP, R. A. 2006 Observation and modelling of barrel droplets on vertical fibres subjected to gravitational and drag forces. *J. Colloid Interface Sci.* **300** (2), 704–712.

MULLINS, B. J., BRADDOCK, R. D., AGRANOVSKI, I. E., CROPP, R. A. & O'LEARY, R. A. 2005 Observation and modelling of clamshell droplets on vertical fibres subjected to gravitational and drag forces. *J. Colloid Interface Sci.* **284** (1), 245–254.

MULLINS, B. J., PFRANG, A., BRADDOCK, R. D., SCHIMMEL, T. & KASPER, G. 2007 Detachment of liquid droplets from fibres-experimental and theoretical evaluation of detchment force due to interfacial tension effects. *J. Colloid Interface Sci.* **312**, 333–340.

QUERE, D., DI MEGLIO, J.-M. & BROCHARD-WYART, F. 1988 Wetting of fibers: theory and experiments. *Rev. Phys. Appl.* **23**, 1023–1030.

DE RUITER, M., DE RUITER, J., ERAL, H. B., SEMPREBON, C., BRINKMAN, M. & MUGELE, F. 2012 Buoyant droplets on functional fibers. *Langmuir* **28**, 13300–13306.

SADER, J., CHON, J. & MULVANEY, P. 1999 Calibration of rectangular atomic force microscopy cantilevers. *Rev. Sci. Instrum.* **70**, 3967–3969.

SAHU, R. P., SINNA-RAY, S., YARIN, A. L. & POURDEYHIMI, B. 2013 Blowing drops off a filament. *Soft Matt.* **9**, 6053–6071.

SAVVA, N. & KALLIADASIS, S. 2013 Droplet motion on inclined heterogeneous substrates. *J. Fluid Mech.* **725**, 462–491.